MAGfect: a novel liposome formulation for MRI labelling and visualization of cells

Morag Oliver,[a] Ayesha Ahmad,[a] Nazila Kamaly,[a] Eric Perouzel,[b] Annabelle Caussin,[b] Michael Keller,[b] Amy Herlihy,[c] Jimmy Bell,[c] Andrew D. Miller*[a,b] and Michael R. Jorgensen*†[a,b]

Received 13th April 2006, Accepted 10th July 2006
First published as an Advance Article on the web 15th August 2006
DOI: 10.1039/b605394g

Cellular entry of imaging probes, such as contrast agents for magnetic resonance imaging (MRI), is a key requirement for many molecular imaging studies, particularly imaging intracellular events and cell tracking. Here, we describe the successful development and *in vitro* analysis of MAGfect, a novel liposome formulation containing a lipidic gadolinium contrast agent for MRI, Gd-DOTA-Chol **1**, designed to enter and label cells. Liposome formulation and cell incubation time were optimised for maximum cellular uptake of the imaging probe in a variety of cell lines. MRI analysis of cells incubated with MAGfect showed them to be highly MRI active. This formulation was examined further for cytotoxicity, cell viability and mechanism of cell labelling. One of the key advantages of using MAGfect as a labelling vehicle arises from its potential for additional functions, such as concomitant drug or gene delivery and fluorescent labelling. The gadolinium liposome was found to be an effective vehicle for transport of plasmid DNA (pDNA) into cells and expression levels were comparable to the commercial transfection agent Trojene™.

Introduction

Molecular imaging can be broadly defined as the *in vivo* characterisation and measurement of biological processes at a cellular or molecular level.[1] Central to this field are the imaging modalities themselves, namely nuclear imaging (positron emission tomography (PET) and single photon emission computed tomography (SPECT)), optical imaging and magnetic resonance imaging (MRI).[2] Although nuclear and optical imaging techniques currently dominate this research field, the attractive safety profile, excellent resolution and long life-time of probes (contrast agents), mean that MRI is proving to be a valuable technique, particularly for the rapid translation of research to a clinical setting.

MRI is a non-invasive imaging technique that allows investigation of opaque organisms in 3D.[3] The images are derived from the NMR signal (behaviour of unpaired nuclear spins in applied magnetic fields) of the protons of water molecules, where the signal intensity in a given volume is a function of both the proton relaxation times (longitudinal T_1 and transverse T_2) and concentration of water.[3,4] This signal intensity can be altered by the presence of contrast agents (compounds possessing a paramagnetic ion core) such as gadolinium(III) (predominantly affecting T_1 relaxation) or iron(III) (predominantly affecting T_2 relaxation) many of which have been FDA approved.[3] Using specific MRI sequences, the exact location of a contrast agent can be pin-pointed within a sample, making these agents particularly interesting for molecular imaging purposes.

Although gadolinium generally displays lower relative sensitivity compared to iron(III)-based contrast agents, it does induce a positive contrast change in the MR images as opposed to iron-induced darkening of images which is often undesirable in biological systems. Thus the choice of contrast agent will depend on the nature of the tissue being studied.

With the increasing amount of attention that cell-based therapies are receiving as potential novel therapeutics, the development of methods to permit non-invasive and repeated *in vivo* whole body cell tracking are becoming highly desirable.[5–8] Indeed, the ability to gain dynamic information concerning the fate and interactions of these transplanted cells within the whole body is critical to its transition to medical practice. Currently cell tracking has become an invaluable tool for studying the movement of cells in animal disease models.[9,10] For example Bulte *et al.*[9] successfully contrast labelled oligodendrocyte progenitors and tracked their migration and subsequent role in neuron remyelination in rats by MRI. The properties of stem cells mean that these cells have received significant attention as potential therapeutics to replace cells lost due to traumatic injury or degenerative disorders, and as such there have been several examples successfully detailing *in vivo* tracking of stem cells in animal models.[11–13] Similarly, tumour imaging has also become an important area of MR imaging and *ex vivo* labelling of cancer cells with suitable contrast agents and the behaviour of the reimplanted cell has been followed by MRI.[14–16]

In order to successfully image cell tracking two main basic requirements must be met: (i) an effective method to label the

[a]*Imperial College Genetic Therapies Centre, Department of Chemistry, Flowers Building, Armstrong Road, Imperial College London, London, UK SW7 2AZ. E-mail: a.miller@imperial.ac.uk; Fax: +44 (0)20 7594 5803; Tel: 44 (0)20 7594 5869*

[b]*IC-Vec Ltd, 13 Prince's Gardens, London, UK SW7 1NA. E-mail: m.jorgensen@imperial.ac.uk; Fax: +44 (0)20 7594 1061; Tel: 44 (0)20 7594 3150*

[c]*Molecular Imaging Group and Biological Imaging Centre, Imaging Sciences Department, MRC Clinical Sciences Centre, Imperial College London, Hammersmith Hospital, London, UK W12 0HS, jimmy.bell@csc.mrc.ac.uk; Fax: +44 (0)20 8383 3038; Tel: 44(0) 20 8383 1517*

† *Present address:* King's College London, 8th Floor, Capital House, 42 Weston Street, London SE1 3QD. Email: michael.jorgensen@kcl.ac.uk; Fax +44 (0)207 848 8122

cells with a suitable probe (long term labelling with minimal cytotoxicity) and (ii) a method to track these cells. To date the majority of cell labelling methods have involved the *ex vivo* labelling of cells *via* either adhering the imaging probe to the cell surface,[17,18] or though its internalisation.[9,11,19,20] Although the former avoids circumnavigating the cell membrane it can create problems though recognition of transplanted cells by the host immune system. As such internalisation of suitable imaging probes, such as gadolinium or iron-based contrast agents for MRI is an attractive prospect. Currently the majority of contrast agents are extracellular and have been designed as blood pool imaging agents.[21,22] However, with the increasing prominence of molecular imaging as a discipline, there has been a few examples of the development of membrane permeable contrast agents.[11,23–29] Despite the successes of these agents they are either limited in their ability to enter cells or to perform additional functions once inside the cell. Our aim was to develop a liposome cell labelling system which would be amenable to labelling a variety of cells, but could also possess additional interesting functions such as delivery of plasmid DNA (pDNA) or other nucleic acid derived therapeutics. An additional aspect is that these liposomes can easily be modified to include a fluorescent label.

Liposomes are artificially constructed spheres of lipid bilayer which enclose an aqueous compartment. The key components of liposomes are the lipids themselves and they control the overall properties of the liposomes. In particular the introduction of cationic lipids (such as CDAN (*N*′-cholesteryloxycarbonyl-3–7-diazanonane-1,9-diamine)[30] or DOTAP (1,2-dioleoyl-3-(trimethylammonio)propane))[31] has been used for the development of liposomes that are designed to enter both primary,[32,33] and classical immortalised cell lines.[34,35]

Here we report on the development of a gadolinium cell labelling liposome using a novel molecule, Gd·DOTA·chol **1** as the key lipid. Gd·DOTA·chol **1** is a cholesterol-based gadolinium chelating lipid that was designed to easily embed into the membranes of standard cationic liposomes. The formulation and cell uptake analysis of a variety of liposomes containing Gd·DOTA·chol **1** are detailed. An optimised formulation, MAGfect, was selected and found to successfully render cells MRI active though a mechanism of cellular uptake. Transfection data with pDNA using the optimised Gd·DOTA·chol **1** liposome is also shown.

Results and discussion

Synthesis of Gd·DOTA·chol (1)

The synthesis of the gadolinium lipid Gd·DOTA·chol **1** is shown in Scheme 1. The reaction between *N*′-cholesteryloxy-3-carbonyl-1,2-diaminoethane **3** and DOTA·NHS·ester **2** proceeds readily at room temperature in the presence of triethylamine. The metal free ligand DOTA·chol **4** was isolated after silica gel column chomatography as a pale water-soluble solid in good yield (76%). The gadolinium complex Gd·DOTA·chol **1** was prepared in high yield by reaction with Gd_2O_3 in water at 90 °C. Any residual ionic impurities were removed using ion exchange resins. Gd·DOTA·chol **1** was isolated as a white solid in excellent yield and purity (as determined by HPLC, ESI-MS and ICP-AES analysis).

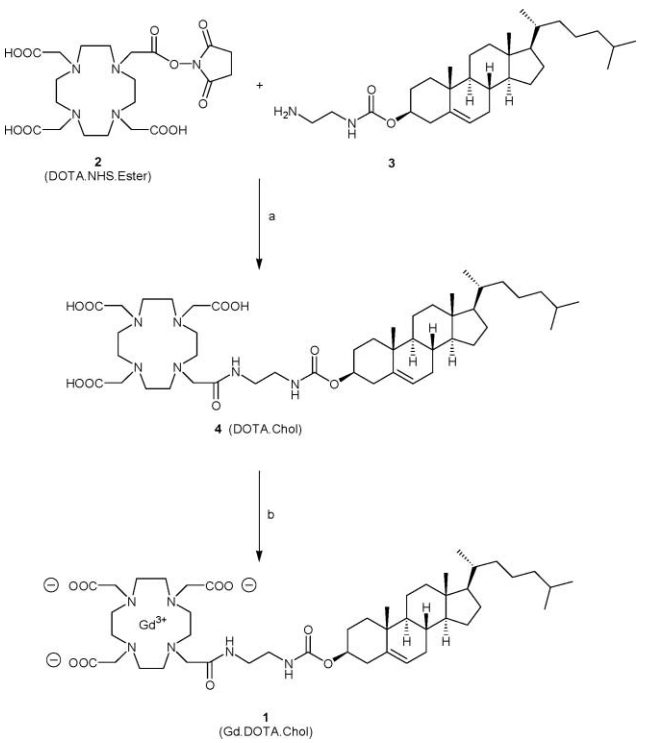

Scheme 1 Synthesis of Gd·DOTA·chol **1** reagents and conditions: (a) $CHCl_3$, NEt_3, RT, 3 h, 76%, (b) Gd_2O_3, H_2O, 90 °C, 12 h, 58%.

MR Activity of gadolinium lipids

The efficacy of Gd·DOTA·chol **1** was assessed by measuring the T_1 relaxation time, T_1 relaxivity and obtaining contrasted MR images of solutions containing the lipid (see Fig. 1 and Table 1). In each case the efficacy of the lipid was compared to that of Gd·DOTA, a clinically used contrast agent (Dotarem™, Guerbet S.A., Fr). MR images provide an excellent visual representation of the efficacy of a given sample and measurement of proton T_1 relaxation times provides a quantitative analysis. An effective gadolinium contrast agent gives rise to a sharp decrease in the T_1 relaxation time, which manifests itself in an increase in the visual signal intensity. The T_1 saturation recovery method was used to determine T_1 values for the different compounds and labelled particles. It is governed by

Table 1 T_1 Relaxation times for Gd·DOTA·chol and appropriate controls (% decrease compared to water)

	Sample	T_1 relaxation/ms	Decrease in T_1 relaxation (%)
1	Water	2937 ± 28	—
2	Gd·DOTA·chol **1**	446 ± 13	85
3	Gd·DOTA	390 ± 8	87

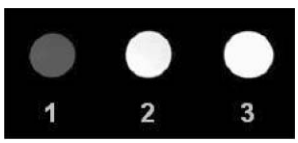

Fig. 1 MR Images of Gd·DOTA·chol **1** and the appropriate controls show the MR activity (bright contrast) of Gd·DOTA·chol lipids. (1. Water, 2. Gd·DOTA·chol, 3. Gd·DOTA).

Table 2 Liposome formulations, associated size and uptake efficiency

CDAN (%)	DOPE (%)	DOTAP (%)	Gd·DOTA·chol (%)	DSPC-Rhodamine	Size/nm	Uptake (%)	GD uptake/μg
20	29.5	—	50	0.5	130	12.3	0.07
20	39.5	—	40	0.5	121	20.7	0.10
40	29.5	—	30	0.5	101	38.2	0.14
35	39.5	—	25	0.5	158	42.4	0.13
30	49.5	—	20	0.5	127	30.5	0.08
60	29.5	—	20	0.5	115	27.9	0.04
50	39.5	—	10	0.5	106	35.1	0.05
—	—	49.5	50	0.5	130	13.1	0.06
—	—	59.5	40	0.5	121	13.2	0.09

eqn 1, where x is the TR value, and S_i is the measured signal for a given TR point.

$$S_i = S_0(1 - e^{(-x/T_1)}) \quad (1)$$

Relaxivity per gadolinium ion was determined by measuring the T_1 of solutions with different concentrations of Gd·DOTA·chol **1** in water. The data is then fit to the following equation

$$R_1\,(C) = 1/T_1(C) + a_1 \times C \quad (2)$$

where $R_1(C)$ is the relaxivity in units $mM^{-1}\ s^{-1}$, and $1/T_1(C)$ is the measured solvent relaxation rate in the presence of Gd·DOTA·chol, with a_1 and C being the T_1 relaxation and concentration values, respectively.

As shown in Fig. 1 and from data in Table 1 it is evident that the novel gadolinium lipid, Gd·DOTA·chol **1** is an effective MRI contrast agent. There is a significant decrease in the T_1 relaxation times and a resultant increase in the observed signal intensity (brightening of the image) compared to that from the control sample (water only). The relaxivity of Gd·DOTA·chol **1**, $4.42 \pm 0.77\ mM^{-1}s^{-1}$, compares well with that of the clinically used contrast agents Dotarem™ and Magnevist™, $5.25\ mM^{-1}\ s^{-1}$.[36] This is an encouraging result which reflects the signal enhancement ability of our novel gadolinium lipid compared to clinical agents.

Towards MAGfect: ascertaining an optimised liposome formulation

Cationic liposomes are readily taken up into cells *via* either endocytosis or membrane fusion. The initial attachment is mediated *via* electrostatic interactions between the slightly negatively charged cell surface and the positively charged liposomes. The ideal cell labelling liposome must be able to facilitate this interaction whilst delivering the maximum amount of gadolinium to the cell.

A series of 9 cationic liposomes were formulated. These formulations were based on either the *N′*-cholesteryloxycarbonyl-3,7-diaza-1,9-diaminonane (CDAN)–dioleoylphosphatidylethanolamine (DOPE) or 1,2-dioleoyloxy-3-(trimethylammonio)propane (DOTAP) systems. The liposomes contained from 20–60 mol% cationic lipid, 10–50 mol% Gd·DOTA·chol **1** and 0.5 mol% DSPE–Rhodamine (as a fluorescent probe for the uptake assays), were sonicated until they were between 100–150 nm in size and titrated until a physiological pH was obtained. The cell labelling efficiency of each formulation was then assessed using the fluorescence cell uptake assay. In brief, the liposomes at various doses were incubated with cultured cells for either 4 or 8 h. After incubation the cells were thoroughly washed and lysed. The lipids taken into the cells were extracted from the cell lysate using a chloroform–methanol mix. The organic extracts were then analysed by fluorescence spectroscopy to quantify the amount of DSPE–Rhodamine, and therefore the amount of liposomes and Gd–lipid taken into cells.

Results, shown in Table 2, indicated that CDAN-based cationic liposomes were more efficient labelling vehicles than DOTAP-based liposomes, and thus, the maximum labelling efficiency was achieved with the MAGfect liposome formulation of 40 mol% CDAN, 30 mol% DOPE and 30 mol% Gd·DOTA·chol **1** (0.14 μg of Gd per 80 000 cells).

To further test the versatility of this liposome formulation, uptake experiments with the optimal MAGfect construct were repeated on MCF-7 and Neuro-2a cell lines. These cell lines were chosen arbitrarily from commonly used cell stocks available in our laboratories. Results from these experiments, in addition to results from the HeLa cell line, are shown in Fig. 2. It is evident that increasing both the liposome–cell incubation time and dose of liposome used results in substantial increases in the total liposome (and subsequently gadolinium label) taken into the cell ($p < 0.05$). However, it was noted that using either a 24 h incubation time or the highest dose of liposome (18 μg of total lipid) often resulted in a substantial amount of cell death. These trends were further verified using ^{14}C uptake protocols, where ^{14}C-cholesterol molecules were incorporated into the liposomes instead of the fluorescent rhodamine lipid and the uptake was quantified with the radioactivity measured in the cell lysate.

Any effective cell labelling vehicle must be able to transfer the label without inferring cytotoxic effects while maintaining an adequate level of cell viability. For these studies, cells were incubated with the liposomes (6, 12 and 18 μg) for 4 and 8 h, washed and allowed to proliferate for an additional 24 h to assess adverse cellular response after liposome incubation. The cytotoxicity of MAGfect *in vitro* was determined using the lactate dehydrogenase (LDH) assay and cell viability was measured using a standard methyl thiazole tetrazolium (MTT) assay. The results showed limited cytotoxicity for all incubation times and liposome doses (<10%), except for the maximum dose of liposomes (18 μg total lipid) with prolonged incubation time. Similarly, MTT viability profiles show 80–90% viability for 4 h incubation and only marginally less for the 8 h incubation period, for both the 6 and 12 μg doses. Decreased viability is observed at the maximum dose. Overall the ideal cell labelling conditions were deduced to be a 12 μg dose of MAGfect with an 8 h incubation time. Here, 30% of MAGfect was taken into cells, corresponding to around 0.07 μg of Gd·DOTA·chol **1** per total cellular content, conferring <4% cytotoxicity and an average of 75% cell viability.

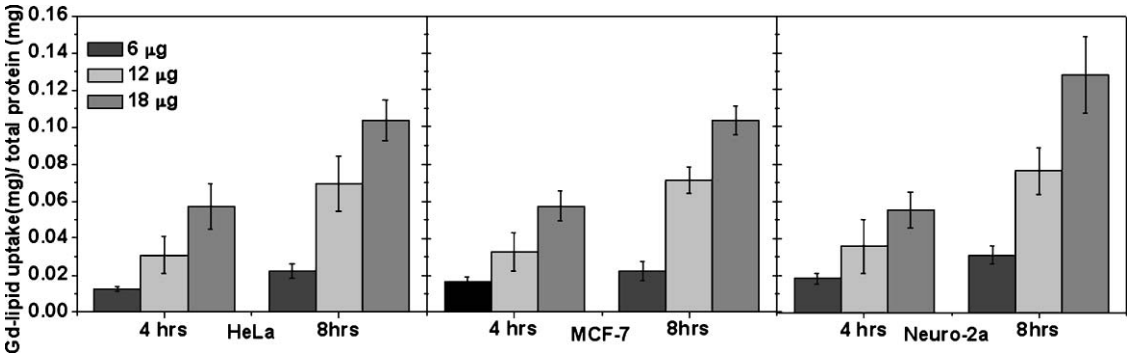

Fig. 2 Relationship between dose of MAGfect liposomes to mass of gadolinium taken up into the cells at 4 and 8 h incubation times, respectively, with optimal liposome formulation for MAGfect: CDAN (40 mol%)–DOPE (30 mol%)–Gd·DOTA·chol **1** (30 mol%). Increase in incubation time and dose results in increased Gd–lipid uptake.

Analysis of labelled cells

Cells treated with the MAGfect gadolinium liposomes were analysed by MRI to see if they were MR visible and efficient contrast agents. For the MRI analysis, 10^6 HeLa cells were labelled (using scaled-up optimised conditions) and harvested. The cells were transferred to an Eppendorf tube and imaged. As controls, cells treated with liposomes containing no gadolinium were also studied. The results of these experiments are shown in Fig. 3 and Table 3.

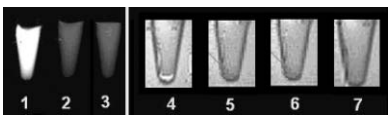

Fig. 3 MR images of gadolinium containing liposomes and cells show positive contrast and, thus, successful cellular labelling. (1) MAGfect gadolinium liposomes (CDAN (40 mol%): DOPE (30 mol%): Gd·DOTA·chol **1** (30 mol%) at 1.2 mg mL^{-1}), (2) control liposomes (CDAN (40 mol%): DOPE (30 mol%): cholesterol (30 mol%) at 1.2 mg mL^{-1}), (3) PBS, (4) cells incubated with MAGfect gadolinium liposomes, (5) cells incubated with control liposomes, (6) control cells (untreated), (7) PBS.

The optimised MAGfect gadolinium liposomes are effective contrast agents (see Fig. 3). There is a clear increase in signal intensity (brightening of the image) with the gadolinium liposomes compared to the control liposomes, which appear dark. Analysis of the T_1 relaxation times for these samples confirms this, with the gadolinium lipids reducing the T_1 relaxation time to 84% of its original value, compared to the control liposomes and PBS alone.

An interesting observation is that the relaxivity (*i.e.*, the potential to shorten the T_1 or T_2 relaxation times of water) of the Gd–liposomes is similar to values obtained for the individual Gd·DOTA·chol lipids themselves. This is unexpected since macromolecular contrast agents, such as liposomes, have been shown to tumble slower designated by a parameter called the rotational correlation time τ which has an effect of increasing the relaxivity (*i.e.*, lower T_1 values).[37] A preliminary analysis of Gd·DOTA·chol by photon correlation spectroscopy (PCS) shows the lipids to have similar sizes to the liposomes, indicating that when dispersed in water they self assemble forming macromolecular structures thus likely accounting for similar relaxivity values calculated for the liposomes. This observation raised further concerns that the Gd·DOTA·chol, when mixed with CDAN and DOPE, may not be forming homogenous liposome assemblies and instead it may be formulating a heterogenous mixture of macrocycles containing mixed ratios of lipid components. In order to investigate this possibility, X-ray studies were performed on the MAGfect liposome mixture. Detection of a single diffraction peak at 20 nm confirmed that indeed a homogenous liposome assembly was being obtained. PCS analysis showed a liposome dispersity size range of 350.7 ± 160 nm.

A series of confocal microscopy experiments were conducted to ascertain a preliminary mechanistic analysis of the cell labelling, *i.e.*, whether the liposomes are entering the cells or merely attached to the cell surface. IGROV-1 cells were grown on glass slides and incubated with fluorescently (0.5 mol% DSPE–Rhodamine) labelled optimised MAGfect for 4 h. After incubation the cells were thoroughly washed (see the Experimental section) to remove any liposomes adhered to the cell surface, and the glass slides were mounted for microscopic analysis. A 3D laser scanning micrograph of a typical image is shown in Fig. 4.

The image shows that the MAGfect liposomes are ubiquitously present within the cytoplasm of the cell, but do not appear to

Table 3 T1 Relaxation times for MAGfect gadolinium liposomes, MAGfect labelled cells and appropriate controls

	Sample	T_1 relaxation/ms	Decrease in T_1 relaxation (%)
1	MAGfect	445 ± 13	84
2	Control liposomes	2763 ± 166	—
3	PBS	2826 ± 174	—
4	Cells incubated with MAGfect	1572 ± 180	45
5	Cells incubated with control liposomes	2624 ± 354	—
6	Cells only	2761 ± 704	—
7	PBS	2826 ± 174	—

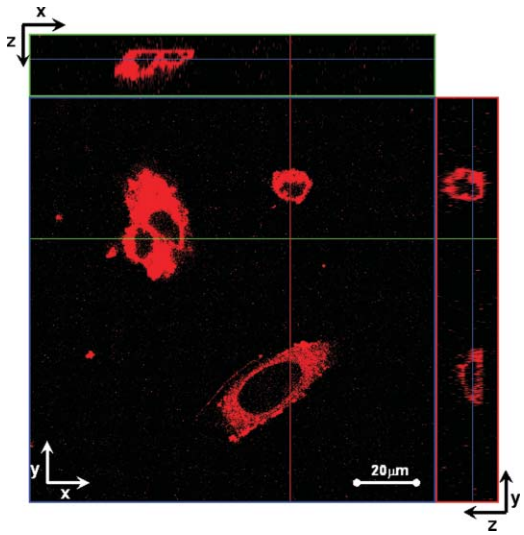

Fig. 4 Laser scanning micrograph projection of cells shows internalization of MAGfect liposomes containing Rhodamine and gadolinium labels.

be in the nucleus. The usage of the fusogenic lipid, DOPE, in the liposomes assists in their cytoplasmic delivery as it promotes endosomal disruption. These results are in agreement to work performed by Keller *et al.* which demonstrated cellular uptake of similar CDAN-based liposome–DNA (LD) complexes.[38]

Transfection with pDNA

One of the principle advantages of using liposomes as a cell labelling vehicle is the potential for delivery of a multi-functional vector into cells. To test the scope of the new optimised gadolinium liposome developed for cell labelling, a series of cell transfections of pDNA (encoding the β-galactosidase reporter gene) were undertaken using MAGfect–pDNA complexes (termed MAGfect LD particles). The *in vitro* cell transfections were performed on HeLa, MCF-7 and Neuro-2a cell lines, and the data gained is reported as β-galactosidase activity, ascertained using a chemoluminescent assay, in relative light units (RLU) per mg of cellular protein (see Fig. 5). Trojene™ (Avanti Polar Lipids, USA) LD particles were used as a benchmark to assess their transfection efficiency.

MAGfect displays comparable transfection efficiencies to the commercially available Trojene™ demonstrating that the transfer and expression of pDNA by gadolinium containing liposomes is therefore not significantly affected by the presence of a gadolinium metal chelate ($p \gg 0.05$). Both the cytotoxicity and the cell viability of both LD particles were assessed as before. No significant unfavourable cellular effects or differences between the two DNA vectors was observed. These preliminary results show that the optimised MAGfect gadolinium cell labelling particle can also mediate transfer of pDNA with no adverse cellular response.

Conclusions

In summary, we have described the development and *in vitro* analysis of MAGfect, a novel liposome formulation containing a lipidic gadolinium contrast agent for MRI designed to enter and label cells. The optimised liposome formulation and labelling conditions were ascertained by examining the effect of variations in lipid formulation, liposome–cell incubation time and liposome

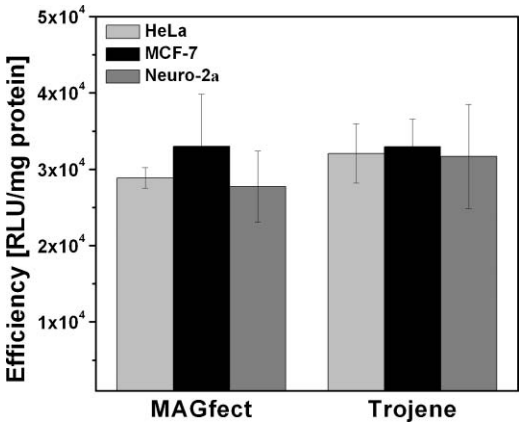

Fig. 5 Transfection with LD systems. MAGfect liposome (CDAN (40 mol%): DOPE (30 mol%): Gd·DOTA·chol (30 mol%)) LD particles, Trojene™ (CDAN (50 mol%): DOPE (50 mol%)) LD particles. All LD particles were formulated with 12 : 1 liposome–DNA ratios (*w*/*w*). Transfections were performed on HeLa, MCF-7 and Neuro-2a cell lines cells (48-well plate, 80 000 cells per well). 0.25 μg of DNA was added per well. No hindrance in efficiency was observed with the incorporation of Gd·DOTA·chol.

dose on uptake of the gadolinium probe into the cells. Using LDH and MTT assays the cytotoxicity and cell viability induced by the optimised liposome was also assessed and found to be minimal (<4%).

MRI analysis of cells incubated with MAGfect under optimised conditions showed them to be highly MRI active, reducing the T_1 relaxation of the cells to <50% of their original values, comparable to other published results.[4] Furthermore our initial mechanistic investigations revealed that the mechanism of labelling proceeds *via* entry of the liposomes into the cells. The liposomes appear to be ubiquitously distributed throughout the cytoplasm, but not within endosomal compartments or the cell nucleus. One of the key advantages of using a liposome based labelling system is the potential for the liposome to possess additional functions, such as delivery of a gene or drug, which would be a valuable tool for molecular imaging. MAGfect was found to be an effective vehicle for transport of pDNA into cells and did not inhibit its expression.

Overall the results detail development of an effective gadolinium cell labelling vehicle to permit MR imaging of cells. The intrinsic make-up of liposomes means they are readily adaptable particles and using these results as a bench-mark it will be possible to further tailor MAGfect to be amenable to label a variety of cell lines. Using previous liposome/stem cell research as a guideline it would be interesting to modify our system for uptake into stem cells. This application would be of great interest for many molecular imaging studies and would provide a valuable imaging tool, which, having been based on clinically approved contrast agents, could be translational to clinical research.

Experimental

Materials

1,2-Dioleoyloxy-3-(trimethylammonio)propane (DOTAP), *N*′-cholesteryloxycarbonyl-3–7-diazanonane-1,9-diamine (CDAN) and DSPE–Rhodamine were obtained from Avanti Polar Lipids

(Alabaster, AL, USA). 1,4,7,10-Tetraazacyclododecane-1,4,7,10-tetraacetic acid mono(*N*-hydroxysuccinimidyl ester) (DOTA·NHS·ester) and 1,4,7,10-tetraazacyclododecane-1,4,7,10-tetraacetic acid (DOTA) were obtained from Macrocyclics (Dallas, TX, USA). CH_2Cl_2 was distilled over P_2O_5. All other chemicals were of analytical grade or the best grade available and purchased from Sigma-Aldrich (UK).

Synthetic chemistry

General procedures. ^1H and ^{13}C NMR spectra were recorded on a Bruker Advance 400, using residual isotopic solvent ($CDCl_3$, δ_H = 7.27 ppm, δ_C = 77.0 ppm; CD_3OD, δ_H = 3.84 ppm, δ_C = 49.05 ppm) as internal reference. For NMR characterisations cholesterol is numbered using the standard format.[38,39] Mass spectra were performed using VG-070B, Joel SX-102 or Bruker Esquire 3000 ESI instruments. IRs were obtained on a JASCO FT/IR-620 infra-red spectrometer. UV spectroscopy was conducted on a Pharmacia Biotech UItrospec 4000 spectrometer at defined wavelengths. Analytical HPLC was conducted on a Hitachi-LaChom L-7150 pump system equipped with a Polymer laboratories PL-ELS 1000 evaporative light scattering detector. HPLC method 1: Vydac C-4 peptide column (4.6 × 250 mm): gradient H_2O (0.1% TFA)–MeCN (0.1% TFA)–MeOH, 0 min [100 : 0 : 0], 1–15 min [0 : 100 : 0], 25 min [0 : 100 : 0], 25.1 min [0 : 0 : 100], 45 min [0 : 0 : 100], 45.1 min [100 : 0 : 0], 55 min [100 : 0 : 0]; flow 1 mL min^{-1}. HPLC method 2: Astec Diol Column (4.6 × 250 mm): solvent mixture A: hexane–isopropanol–glacial acetic acid–triethylamine (101 : 21 : 2 : 0.1 by volume); solvent mixture B: isopropanol–water–glacial acetic acid–triethylamine (105 : 17.5 : 2 : 0.1); gradient 0 min [95% A–5% B], 20 min [0% A–100% B], 23 [95% A–5% B], 45 min [95% A–5% B]; flow 1 mL min^{-1}.

1,4,7,10-Tetraazacyclododecane-1,4,7,10-tetraacetic acid mono-(*N*′-cholesteryloxy-3-carbonyl-1,2-diaminoethane)amide (DOTA·chol; 4). DOTA·NHS·ester 2 (75 mg, 0.15 mmol) was dissolved in dry chloroform (40 mL). *N*′-Cholesteryloxy-3-carbonyl-1,2-diaminoethane (70.7 mg, 0.15 mmol) and triethylamine (415 μL, 302 mg, 2.99 mmol) were added to the solution.[40] The reaction was stirred at room temperature under argon until TLC indicated completion (~3 h). The solvents were removed *in vacuo* and the resulting residue purified by silica gel column chomatography [CH_2Cl_2–MeOH–NH_3 92 : 17 : 1 → CH_2Cl_2–MeOH–NH_3 75 : 32 : 3], giving the title compound **4** (97 mg, 76%) as a pale yellow solid. FTIR (nujol) ν_{max} 3139, 2919, 2725, 1708, 1589, 1459, 1405, 1376, 1154, 1092, 1013 cm^{-1}; ^1H NMR (MeOD) 0.71 (3 H, s, 18-CH_3), 0.86–0.87, 0.86–0.88 (2 × 3 H, d, J = 6.4 Hz, overlapping 1.2 Hz, 27-CH_3, 26-CH_3), 0.93–0.94 (3 H, d, J = 6.4 Hz, 21-CH_3), 1.02 (3 H, s, 19-CH_3), 1.04–1.64 (21 H, m, 1-CH_2, 9-CH, 11-CH_2, 12-CH_2, 14-CH, 15-CH_2, 16-CH_2, 17-CH, 20-CH, 22-CH_2, 23-CH_2, 24-CH_2, 25-CH), 1.81–2.09 (5 H, m, 2-CH_2, 7-CH_2, 8-CH), 2.27–2.34 (2 H, m, 4-CH_2), 2.50–3.10 (22 H, m, 3′-CH_2, 4′-CH_2, 7′-CH_2, 4 × NCH_2CH_2N), 3.10–3.56 (8 H, m, 3 × CH_2COOH), 4.34–4.39 (1 H, m, 3-CH), 5.33–5.39 (1 H, m, 6-CH); ^{13}C NMR (MeOD) 12.4 (18-CH_3), 19.3 (21-CH_3), 19.8 (19-CH_3), 22.2 (11-CH_2), 23.0 (27-CH_3), 23.2 (26-CH_3), 25.0 (23-CH_2), 25.4 (15-CH_2), 26.4 (16-CH_2), 29.2 (25-CH), 29.4 (2-CH_2), 33.1 (8-CH) 33.3 (7-CH_2), 37.1 (20-CH), 37.4 (22-CH_2), 37.8 (10-C), 38.3 (1-CH_2), 39.8 (24-CH_2), 40.6 (4′-CH_2), 40.7 (4-CH_2), 41.1 (3′-CH_2), 41.2 (12-CH_2), 43.5 (13-C), 51.7 (9-CH), 54.22 (br, NCH_2CH_2N × 4), 57.6 (17-CH), 58.1 (7′-CH_2), 58.2 (14-CH), 60.2 (2 × CH_2COOH), 60.4 (1 × CH_2COOH), 75.7 (3-CH), 123.5 (6-CH), 141.3 (5-C), 158.8 (1′-CO), 175.1 (6′-CO), 179.8 (2 × CH_2COOH), 179.9 (1 × CH_2COOH); *m/z* (FAB +ve) 859 (M + H); FAB-MS *m/z* for $C_{46}H_{78}N_6O_9K$ (M + K) calculated 897.5467, found 897.5487; HPLC analysis-method 1: R_t = 24.5 min; method 2: R_t = 21.95 min.

Gadolinium(III) 1,4,7,10-tetraazacyclododecane-1,4,7,10-tetraacetic acid mono(*N*′-cholesteryloxy-3-carbonyl-1,2-diaminoethane)amide (Gd·DOTA·chol; 1). DOTA·cholesterol 4 (50 mg, 0.058 mmol) was dissolved in water (10 mL). Gadolinium oxide (8 mg, 0.029 mmol (1 eq. per Gd)) was added to the solution, forming a cloudy suspension. The reaction mixture was heated to 90 °C for 12 h. The solution was cooled to room temperature and to it were added cation-exchange resin (Amberlite IR 12/H^+-form) and anion-exchange resin (Amberlite IRA 67/OH ··· form). After stirring for 60 min at ambient temperature, the resin was collected by filtration though 0.22 μm filters. The filtrate was removed by freeze-drying rendering the title compound **1** (35 mg, 58%) as a pale yellow solid. The xylenol orange test showed an absence of free gadolinium ions. IR (nujol) ν_{max} 3137, 2918, 1599, 1458, 1403, 1376, 1319, 1244, 1156, 1084, 1002 cm^{-1}; *m/z* (ESI +ve) 1014 (M^+); HPLC analysis method 1: R_t = 25.5 min; method 2: R_t = 23.75 min.

N.B. The mass spectrum shows the complex with all abundant isomers of gadolinium bound.

Gadolinium(III) 1,4,7,10-tetraazacyclododecane-1,4,7,10-tetraacetic acid (Gd·DOTA). DOTA (50 mg, 0.123 mmol) was dissolved in water (10 mL). Gadolinium oxide (22 mg, 0.0618 mmol, 0.5 eq. (1 eq. per Gd)) was added to the solution, forming a cloudy suspension. The reaction mixture was heated to 90 °C for 12 h, upon which the solution was clear. The xylenol orange test showed there was no free gadolinium in solution. The reaction was cooled to room temperature and to it were added cation-exchange resin (Amberlite IR 12/H+-form) and anion-exchange resin (Amberlite IRA 67/OH-form). After stirring for 60 min at ambient temperature, the resin was collected by filtration though 0.22 μm filters. The filtrate was removed by freeze-drying rendering the title compound (42 mg, 61%) as a white shiny powder (mp > 260 °C). The xylenol orange test showed that there was no free gadolinium present: FTIR (nujol mull) ν_{max} 3401, 2976, 2876, 2828, 1658, 1630, 1551, 1468, 1409 cm^{-1}; *m/z* (ESI +ve) 558 (M^+), 279 ($2M^+$); HPLC analysis-method 1: R_t = 3.5.

N.B. Mass spectrum shows the complex with all abundant isomers of gadolinium bound.

MRI analysis of Gd·DOTA·chol

Gd·DOTA·chol **1** and Gd·DOTA (and controls of the metal free compounds) were dissolved in appropriate solvents to give a final concentration of 0.5 mM. The solutions (200 μL) were placed in Eppendorf tubes and imaged at 4.7 *T*, spin echo sequence: T_R = 50, 100, 200, 300, 500, 700, 1200, 3000, 5000, 7000 ms, T_E = 15 ms, number of signal averages = 2, 1 slice coronal (2 mm thick). FOV; 70 × 70 mm^2, collected into a matrix of 256 × 128. To ensure a fair comparison of the efficacy of each compound, blank tubes containing the respective compounds solvents were also imaged.

Relaxivity analysis of Gd·DOTA·chol

T_1 values were obtained using the method described above for five concentrations of Gd·DOTA·chol **1**: 1.724960, 1.508108, 1.181876, 0.8871224, 0.4769475 mM, and the relaxivity was calculated using eqn 2.

Liposome formulation

All lipids were stored as stock solutions in anhydrous organic solvents ($CHCl_3$, MeOH or mixture of both), at −20 °C under argon. Liposomes were made with a variety of defined molar ratios of individual lipids to give a defined total lipid concentration of 1.2 mg mL^{-1} in water. Fluorescent liposomes always contained 0.5 mol% DSPE–Rhodamine as a fluorophore.

Appropriate volumes of each lipid stock were placed in a round bottom flask (typically 10 mL) containing distilled CH_2Cl_2 (1 mL) and stirred to ensure thorough mixing of the lipids. The solvent was slowly removed *in vacuo* to ensure production of an even lipid film. The film was re-hydrated with water (defined volume). The resulting solution was sonicated for 1–10 min, in order to form liposomes of appropriate size. The pH of the liposomal suspension was checked by pH Boy (Camlab Ltd., Over, Cambridgeshire, UK) and if appropriate adjusted to neutral by addition of aqueous solutions of NaOH and HCl. For each preparation, the size distribution of liposomes was measured by photon correlation spectroscopy (PCS) to ensure a size distribution of below 200 nm. MAGfect liposomes were one-phase as verified by small angle X-ray diffraction.

In vitro fluorescent cell uptake assay

Twenty four hours prior to liposome uptake, adherent HeLa, MCF-7 and Neuro-2a cells were grown in Dulbecco's modified Eagle culture medium (DMEM) with 10% fetal calf serum and 1% penicillin–streptomycin (Sigma), in a 48-well plate (80,000 cells per well, 250 μL of complete medium) and in a wet (37 °C) 10% CO_2–90% air atmosphere. The cells were grown until 80% confluent. The media was then removed and replaced with fresh media (same volume as previous). Fluorescent liposomes (6 μg (5 μL of 1.2 mg mL^{-1} liposomes), 12 μg (10 μL of 1.2 mg mL^{-1} liposomes) or 18 μg (15 μL of 1.2 mg mL^{-1} liposomes) doses were then added to each well, swirled to ensure even dispersion and then incubated in a wet (37 °C) 10% CO_2–90% air atmosphere for either 4, 8 or 24 h.

After liposome uptake the cells were washed with PBS (2 × 200 μL) and then treated with lysis buffer (100 μL per well). Cell lysate (50 μL) was diluted with MeOH (50 μL) and $CHCl_3$ (300 μL). The resulting solution was vigorously vortexed and then allowed to separate into 2 phases (organic and aqueous). The organic layer was isolated and its fluorescence was recorded on a RF-5301PC Shimadzu spectrofluorophotometer (λ_{ex} 535 nm, λ_{em} 580 nm). As a positive control, liposomes (6, 12 or 18 μg) were added to the lysate of untreated cells, providing a 100% liposome uptake result. As a negative control, liposomes (6, 12 or 18 μg for a 48 well plate) were added to wells containing no cells. These should be eliminated during the PBS washing step, providing a baseline liposome uptake result.

The amount of cellular protein was quantified in a BCA assay (Pierce, Rockford, IL, USA) using 10 μL of the cell lysate or bovine serum albumin as internal calibration standard and adding 100 μL of BCA reagent (according to suppliers protocol). Following a period of 30 min, the colorimetric measurement was performed at 570 nm by means of a microplate reader (Anthos Lucy 1). Uptake studies were normalized to total cellular protein. Statistical analysis was performed using a two-tailed T-test.

In vitro ^{14}C-cholesterol cell uptake assay

Cells were prepared and transfected in a similar manner shown above except liposomes containing traces of ^{14}C-cholesterol were used. Cellular lysates were then treated with solvable and hydrogen peroxide to ensure cellular breakdown. Standard scintillation counting techniques were used to assess the radioactivity of the samples and normalized to total cellular protein content using a standard BCA assay.

Lactate dehydrogenase toxicity assay (liposomes and liposome–DNA complexes; LD systems)

The CytoTox-96 assay (Promega, Madison, WI, USA) evaluates cellular cytoxicity by assessing the release of lactate dehydrogenase (LDH) into culture medium as a consequence of damaged cell membranes compared to total LDH present in the cells.

Twenty four hours prior to the assay, adherent HeLa cells were grown in Dulbecco's modified Eagle culture medium (DMEM) with 10% fetal calf serum and 1% penicillin–streptomycin (Sigma), in a 48-well (3.5×10^4 cells per well, 250 μL of complete medium) plates and in a wet (37 °C) 10% CO_2–90% air atmosphere. The cells were grown until 80% confluent. The media was then removed and replaced with fresh media (same volume as previous). Liposomes (6, 12 or 18 μg doses) or LD mixtures (10 μL (12.5 μg of DNA) dose) were then added to each well, swirled to ensure even dispersion and then incubated at in a wet (37 °C) 10% CO_2–90% air atmosphere for either (a) liposomes: 4 h, 4 (24) h, 8, 8 (24) h or 24 h; (b) LDs: 3 (24) h.

Measuring LDH release. Growth media (200 μL) from each well was transferred into a 96 well plate and centrifuged (3600 rpm for 10 min). The resulting supernatant (50 μL) was transferred to a white 96 well plate (Corning Costar). Reconstituted substrate mix (50 μL) (made as directed in manufacturers protocol) was added to each well. The plate was placed in an opaque box and incubated for 30 min at room temperature. Stop solution (50 μL) was added to each well and the absorbance at 490 nm was measured by means of a microplate reader (Anthos Lucy 1).

Measuring cell internal LDH. Growth media was removed from each well and the cells were washed with PBS. Lysis buffer (250 μL) was added to each well. Cell lysate (50 μL) was transferred to a white 96 well plate (Corning Costar). Reconstituted substrate mix (50 μL) (made as directed in manufacturers protocol) was added to each well. The plate was placed in an opaque box and incubated for 30 min at room temperature. Stop solution (50 μL) was added to each well and the absorbance at 490 nm was measured by means of a microplate reader (Anthos Lucy 1). Cytoxicity was calculated as a ratio LDH released *versus* total LDH content.

MTT cell viability studies

HeLa, MCF-7 and Neuro-2a cells were seeded at 80 000 cells per well (48 well plate). Cells were incubated with liposomes (6, 12 and 18 μg), prepared as described earlier, for 4 and 8 h, and washed twice with PBS. Cells were allowed to grow for an additional 24 h and a cell proliferation kit (MTT; Roche) assay was used to assess the cells viability post liposome exposure.

MRI analysis of cells

Twenty four hours prior to liposome uptake, adherent HeLa cells were grown in Dulbecco's modified Eagle culture medium (DMEM) with 10% fetal calf serum and 1% penicillin–streptomycin (Sigma), in a 6-well plate (2.5×10^5 cells per well, 3 mL of growth medium) plates and in a wet (37 °C) 10% CO_2–90% air atmosphere. The cells were grown until 80% confluent. The media was then removed and replaced with fresh media (same volume as previous). Gd·liposomes (173 μg dose (144 μL of 1.2 mg mL^{-1} liposomes)) were then added to each well, swirled to ensure even dispersion and then incubated in a wet (37 °C) 10% CO_2–90% air atmosphere for 8 h.

After liposome uptake the cells were washed with PBS (2 × 2 mL) and then treated with trypsin–EDTA (200 μL, 0.25% trypsin, 1 mM EDTA) for 1 min at 37 °C. DMEM (complete, 2 mL) was added to neutralise the trypsin. The cells were counted and 1×10^6 were washed with PBS and then centrifuged in PBS buffer (1 mL) into a pellet in an Eppendorf tube.

The Eppendorf tubes were immersed in a water bath and imaged at 4.7 T, spin echo sequence: $T_E = 12.9$ ms; $T_R = 200$ ms; number of signal averages = 64; single sagital slice 10 mm thick; field of view 100 × 100 mm, collected into a matrix of 256 × 256. The T_1 values of Gd·DOTA·chol solutions in water were determined using the following spin echo sequence: $T_E = 15$, $T_R = 50$, 100, 200, 300, 500, 700, 1200, 3000, 5000, 7000 ms; number of signal averages = 4; single sagital slice with 2 mm thickness; FOV; 100 × 100 mm collected into a matrix of 256 × 125. As negative controls; cells treated with liposomes containing no Gd·lipid (substituted for cholesterol), untreated cells and an Eppendorf containing PBS buffer were imaged.

Laser scanning confocal microscopy

Twenty four hours prior to liposome uptake, adherent IGROV-1 cells were grown in Dulbecco's modified Eagle culture medium (DMEM) with 10% fetal calf serum (FCS, sigma) and 1% penicillin–streptomycin (Sigma), in 6-well (2.5×10^5 cells per well, 3 mL of complete medium) plates fitted with glass slides, in a wet (37 °C) 10% CO_2–90% air atmosphere. The cells were grown until 80% confluent. The media was then removed and replaced with fresh media (same volume as previous). Fluorescent liposomes (173 μg (144 μL of 1.2 mg mL^{-1} liposomes) per well) were then added to appropriate wells, swirled to ensure even dispersion and then incubated in a wet (37 °C) 10% CO_2–90% air atmosphere for 4 h.

After liposome uptake the media was removed and the cells were washed with PBS (× 2), heparin (× 1 (20 mg mL^{-1})), PBS (× 2), PFA (× 1 (20 min at 37 °C)), PBS (× 2), glycine (× 1 (20 mM, 20 min at 37 °C)), PBS (× 2). The glass slides were removed from the wells and fixed to microscopy slides. Confocal images were taken on an upright Zeiss LSM 510 microscope

Liposome–DNA *in vitro* transfection studies

Complex formation. pDNA containing the β-galactosidase gene (pNGVL1-nt-beat-gal 7.53 kbp) was stored as frozen aliquots at −80 °C, at a concentration of 1.2 mg mL^{-1}. LD complexes were made by addition of DNA to a continuously vortexing solution of cationic liposomes (1.2 mg mL^{-1} total lipid concentration) to give a final ratio of 12 : 1 (*w*/*w*) liposome to DNA. The size distribution was measured by PCS (Coulter N4 Plus).

LD transfection. Twenty four hours prior to transfection, adherent HeLa, MCF-7, and Neuro-2a cells were grown in Dulbecco's modified Eagle culture medium (DMEM) with 10% fetal calf serum (FCS, sigma) and 1% penicillin–streptomycin (Sigma), in 48-well (3.5×10^4 cells per well, 250 μL of complete medium) plates and in a wet (37 °C) 10% CO_2–90% air atmosphere. The cells were grown until 80% confluent. The media was then removed and replaced with fresh media (same volume as previous).

LD mixtures (0.25 μg of pDNA) were added to each well, swirled to ensure even distribution, and then incubated in a wet (37 °C) 10% CO_2–90% air atmosphere for 3 h. The media was removed, the cells washed with PBS and then replaced with fresh media (250 μL). The cells were then incubated for a further 24 h. Before β-galactosidase activity was measured the cells were washed with PBS and harvested with lysis buffer (150 μL).

β-Galactosidase and total protein assays. After lysis, equal amounts, 50 and 20 μL, of each cell suspension were used for determination of β-galactosidase activity and total cellular protein (to normalise results), respectively.

In the β-galactosidase assay, 100 μL of the substrate reagent was added to 50 μL of the cell suspension in a white 96 well plate (Corning Costar). The plate was incubated for 30 min at room temperature. Automatic initiation was performed by a microplate luminometer (Anthos Lucy 1, Labtech International Ltd., Rigmer, East Sussex, UK) which injected 50 μL initiation reagent and enzymatic activity was measured over the subsequent 30 s. β-Galactosidase activity was normalised by the results of the total protein measured by a standard BSA assay as described above, and expressed as RLU (relative light units) per mg of protein.

Acknowledgements

Dr Morag Oliver gratefully acknowledges funding from IC-Vec, Ltd. Funding for Dr Ayesha Ahmad provided by National Science Foundation, USA, IRFP grant. The authors would also like to acknowledge the MRC for financial support and the Biological Imaging Centre, Imaging Sciences Department, Imperial College London and the Wellcome Trust for the use of the MRI facility and Juan Miguel Mura Morales.

References

1 R. Weissleder and U. Mahmood, *Radiology*, 2001, **219**, 316–333.
2 H. R. Herschman, *J. Nucl. Cardiol.*, 2004, **11**, 210–214.

3 R. J. M. van Geuns, P. A. Wielopolski, H. G. de Bruin, B. J. Rensing, P. M. A. van Ooijen, M. Hulshoff, M. Oudkerk and P. J. de Feyter, *Prog. Cardiovasc. Dis.*, 1999, **42**, 149–156.
4 M. J. Allen, K. W. MacRenaris, P. N. Venkatasubramanian and T. J. Meade, *Chem. Biol.*, 2004, **11**, 301–307.
5 S. Agrawal and D. V. Schaffer, *Trends Biotechnol.*, 2005, **23**, 78–83.
6 R. Cancedda, G. Bianchi, A. Derubeis and R. Quarto, *Stem Cells*, 2003, **21**, 610–619.
7 J. K. Fraser, R. E. Scheiber, P. A. Zuk and M. H. Hedrick, *Int. J. Biochem. Cell Biol.*, 2004, **36**, 658–666.
8 M. H. Dahlke, F. C. Popp, S. Larsen, H. Schlitt and J. E. J. Rasko, *Liver Transplant*, 2004, **10**, 471–479.
9 J. W. M. Bulte, S. C. Zhang, P. van Gelderen, V. Herynek, E. K. Jordan, I. D. Duncan and J. A. Frank, *Proc. Natl. Acad. Sci. U. S. A.*, 1999, **96**, 15256–15261.
10 M. Bendszus and G. Stoll, *J. Neurosci.*, 2003, **23**, 10892–10896.
11 M. Modo, K. Mellodew, D. Cash, S. E. Fraser, T. J. Meade, J. Price and S. C. R. Williams, *NeuroImage*, 2004, **21**, 311–317.
12 D. L. Kraitchman, A. W. Heldman, E. Atalar, L. C. Amado, B. J. Martin, M. F. Pittenger, J. M. Hare and J. W. M. Bulte, *Circulation*, 2003, **107**, 2290–2293.
13 G. A. Walter, K. S. Cahill, J. Huard, H. S. Feng, T. Douglas, H. L. Sweeney and J. W. M. Bulte, *Magn. Reson. Med.*, 2004, **51**, 273–277.
14 W. J. Mulder, G. J. Strijkers, J. W. Habets, E. J. Bleeker, D. W. Van Der Schaft, G. Storm, G. A. Koning, A. W. Griffioen and K. Nicolay, *FASEB J.*, 2005, **19**, 2008–2010.
15 Z. Zhang, E. J. Van Den Bos, P. A. Wielopolski, M. de Jong-Popijus, M. R. Bernsen, D. J. Dunker and G. P. Krestin, *Magn. Reson. Mater. Phys., Biol. Med.*, 2005, **18**, 175–185.
16 D. Granon, L. A. Kunz-Schughart and M. Neeman, *Magn. Reson. Med.*, 2005, **54**, 789–797.
17 A. K. Gupta and A. S. G. Curtis, *Biomaterials*, 2004, **25**, 3029–3040.
18 T. Suwa, S. Ozawa, M. Ueda, N. Ando and M. Kitajima, *Int. J. Cancer*, 1998, **75**, 626–634.
19 W. J. M. Mulder, G. J. Strijkers, A. W. Griffioen, L. van Bloois, G. Molema, G. Storm, G. A. Koning and K. Nicolay, *Bioconjugate Chem.*, 2004, **15**, 799–806.
20 M. Zhao, M. F. Kircher, L. Josephson and R. Weissleder, *Bioconjugate Chem.*, 2002, **13**, 840–844.
21 D. D. Schwert, J. A. Davies and N. Richardson, *Top. Curr. Chem.*, 2002, **222**, 165–199.
22 H. Gries, *Top. Curr. Chem.*, 2002, **222**, 1–24.
23 M. J. Allen and T. J. Meade, *JBIC, J. Biol. Inorg. Chem.*, 2003, **8**, 746–750.
24 S. Heckl, J. Debus, J. Jenne, R. Pipkorn, W. Waldeck, H. Spring, R. Rastert, C. W. von der Lieth and K. Braun, *Cancer Res.*, 2002, **62**, 7018–7024.
25 P. Wunderbaldinger, L. Josephson and R. Weissleder, *Bioconjugate Chem.*, 2002, **13**, 264–268.
26 R. Bhorade, R. Weissleder, T. Nakakoshi, A. Moore and C. H. Tung, *Bioconjugate Chem.*, 2000, **11**, 301–305.
27 M. Lewin, N. Carlesso, C. H. Tung, X. W. Tang, D. Cory, D. T. Scadden and R. Weissleder, *Nat. Biotechnol.*, 2000, **18**, 410–414.
28 L. Josephson, C. H. Tung, A. Moore and R. Weissleder, *Bioconjugate Chem.*, 1999, **10**, 186–191.
29 J. F. Kayyem, R. M. Kumar, S. E. Fraser and T. J. Meade, *Chem. Biol.*, 1995, **2**, 615–620.
30 M. Keller, M. R. Jorgensen, E. Perouzel and A. D. Miller, *Biochemistry*, 2003, **42**, 6067–6077.
31 L. Ciani, S. Ristori, L. Calamai and G. Martini, *Biochim. Biophys. Acta*, 2004, **1664**, 70–79.
32 M. T. G. da Cruz, S. Simoes and M. C. P. de Lima, *Exp. Neurol.*, 2004, **187**, 65–75.
33 A. Hamm, N. Krott, I. Breibach, R. Blindt and A. K. Bosserhoff, *Tissue Eng.*, 2002, **8**, 235–245.
34 G. A. Koning, H. W. M. Morselt, J. Kamps and G. L. Scherphof, *J. Liposome Res.*, 2001, **11**, 195–209.
35 A. Gray, D. J. Landfair and M. E. Wiles, *Drug Delivery*, 1999, **6**, 213–226.
36 J. Feng, G. Sun, F. Pei and M. Liu, *Bioorg. Med. Chem.*, 2003, **11**, 3359–3366.
37 W. J. Mulder, G. J. Strijkers, G. A. van Tilborg, A. W. Griffioen and K. Nicolay, *Nucl. Magn. Reson. Biomed.*, 2006, **19**, 142–64.
38 M. Keller, R. P. Harbottle, E. Perouzel, M. Colin, L. Shah, A. Rahim, L. Vaysse, A. Bergau, S. Moritz, C. Brahimi-Horn, C. Coutelle and A. D. Miller, *ChemBioChem*, 2003, **4**, 286–298.
39 E. Perouzel, M. R. Jorgensen, M. Keller and A. D. Miller, *Bioconjugate Chem.*, 2003, **14**, 884–898.
40 J. E. Waterhouse, R. P. Harbottle, M. Keller, K. Kostarelos, C. Coutelle, M. R. Jorgensen and A. D. Miller, *ChemBioChem*, 2005, **6**, 1212–1223.